Postprint of: Biomaterials Volume 32, Issue 29, October 2011, Pages 7263–7273

Mannosyl-coated nanocomplexes from amphiphilic cyclodextrins and pDNA for site-specific gene delivery

Alejandro Díaz-Moscoso (a), Nicolas Guilloteau (b), Céline Bienvenu (b), Alejandro Méndez-Ardoy (c), José L. Jiménez Blanco (c), Juan M. Benito (a), Loïc Le Gourriérec (b), Christophe Di Giorgio (b), Pierre Vierling (b), Jacques Defaye (d), Carmen Ortiz Mellet (c), José M. García Fernández (a)

(a) Instituto de Investigaciones Químicas, CSIC – Universidad de Sevilla, Américo Vespucio 49, Isla de la Cartuja, E-41092 Sevilla, Spain

(b) LCMBA UMR 6001, Université de Nice Sophia Antipolis – CNRS, 28, Avenue de Valrose, F-06100 Nice, France

(c) Departamento de Química Orgánica, Facultad de Química, Universidad de Sevilla, C/ Prof. García González 1, E-41012 Sevilla, Spain

(d) Dépt. de Pharmacochimie Moleculaire, Institut de Chimie Moléculaire de Grenoble (CNRS – Univ. de Grenoble, UMR 5063, FR 2607), Bât. E André Rassat, BP 53, F-38041 Grenoble, France

Abstract

Fully homogeneous facial amphiphiles consisting in a cyclodextrin (CD) platform onto which a polycationic cluster and a multi-tail hydrophobic moiety have been installed (polycationic amphiphilic CDs; paCDs) self-organized in the presence of plasmid DNA to form nanometric complexes (CDplexes) which exhibit broad-range transfection capabilities. We hypothesized that biorecognizable moieties located at the hydrophilic rim in the CD scaffold would be exposed at the surface of the corresponding nanoparticles after DNA-promoted aggregation, endowing the system with molecular recognition abilities towards cell receptors. This concept has been demonstrated by developing an efficient synthetic strategy for the preparation of multivalent polycationic glyco-amphiphilic CDs (pGaCDs). Self-assembled nanoparticles obtained from mannosylated pGaCDs and pDNA (average hydrodynamic diameter 80 nm) have been shown to be specifically recognized by mannose-specific lectins, including concanavalin A (Con A) and the human macrophage mannose receptor (MMR). Further macrophage adhesion studies indicated that unspecific binding, probably due to electrostatic interactions with negatively charged cell membrane components, can also operate. The relative specific versus non-specific internalization is dependent on the pGaCD:pDNA proportion, being optimal at a protonable nitrogen/phosphate (N/P) ratio of 5. The resulting GlycoCDplexes were shown to specifically mediate transfection in Raw 264.7 (murine macrophage) cells expressing the mannose-fucose receptor in vitro. FACS experiments confirmed that transfection using these nanoparticles is mannose-dependent, supporting the potential of the approach towards vectorized gene delivery.

Highlights

► Monodisperse polycationic amphiphilic cyclodextrins (paCDs) efficiently complex pDNA. ► Mannosyl-paCD:pDNA nanocomplexes (Man-CDplexes) are recognized by specific lectins. ► Man-CDplexes adhere to macrophages via the macrophage mannose receptor (MMR). ► MMR-mediated and non-specific internalization take place in RAW 264.7 cells. ► Selective transfection of macrophages was achieved by adjusting the N/P ratio.

Keywords

Carbohydrates; Cyclodextrins; Lectins; Nonviral gene delivery; Self-assembled nanoparticles

1. Introduction

Gene therapy, which implies introduction of genes into cells to prevent or cure a wide range of genetic or acquired diseases, represents nowadays an extremely active domain of research. Successful delivery of genetic materials is dependent on the design of efficient technologies allowing compaction, protection, cell internalization and final release of the nucleic acid payload. Viral vectors have proved very effective in achieving highly efficient gene delivery and expression in vitro; however, this approach early met with severe limitations in terms of immunogenicity and toxicity issues in clinical trials [1]. Research on synthetic gene delivery systems has subsequently gained an increasing relevance due to advantages with regard to non-immunogenicity, scaling-up production and potential for delivery of large DNA fragments into target cells [2]. Among nonviral vectors, cationic polymers and lipids hold a prominent position, both capable of complexing DNA into nanocondensates (polyplexes and lipoplexes, respectively) featuring improved pharmacokinetics and pharmacodynamics [3] and [4]. The overall positive surface electrostatic potential of those mixed nanoparticles promote adhesion to negatively charged cell membrane components (e.g. proteoglycans or glycosaminoglycans), thus enhancing cellular uptake and transfection efficiency [5] and [6]. This mechanism is, however, inherently unspecific and may turn into a hurdle for the delivery of therapeutically relevant gene drugs to specific cell types or tissues.

Varying the nature of small cationic molecule-end groups in linear polymers has been shown to bear some potential to modulate cell-type gene delivery efficiency due to changes in particle-uptake kinetics and/or the polymer-DNA binding interactions that regulate DNA release [7]. Incorporation of structural elements designed to impart targeting abilities to the gene vector architecture or its complexes, including vitamins, carbohydrates, peptides, growth factor or antibodies, has been further explored as a way to engineer artificial viruses, achieve site-specific delivery and prevent side effects [8], [9], [10] and [11]. The intrinsic polydispersity and random conformations of these formulations represent an obstacle for structure–activity relationship (SAR) studies and vector optimisation, however.

Recently, multifunctional macrocyclic platforms [12], such as calixarenes [13] and [14] or cyclodextrins [15], [16], [17], [18] and [19], have emerged as suitable tools to build up monodisperse macromolecular constructs with the potential to condense DNA into transfectious nanoparticles. Polycationic amphiphilic CDs (paCDs; Fig. 1, left) have shown significant promise towards this goal [20], [21], [22] and [23]. These jelly-fish-like molecules, accessible from commercial CDs through face-selective functionalization methodologies, self-organize in the presence of pDNA to form small (40–70 nm) complexes (CDplexes) that mediate transfection with remarkable efficiency. In principle, biorecognizable epitopes installed onto the hydrophilic rim in paCDs would be exposed at the surface of the corresponding CDplexes, provided that the self-assembling process is not disrupted. In the

presence of the putative receptors, the formation of ternary complexes paCD:pDNA:receptor would take place, which can elicit selective internalization routes. Glycoconjugates are particularly appealing tools for this purpose. Similarly to polyethyleneglycol (PEG), glyco-coating usually shields non-specific interactions of cationic surfaces by improving solvation. Additionally, glycoconjugates can be recognized with exquisite specificity by cell membrane receptors (lectins) whose expression depends not only in cell type but also in cell state [24] and [25]. To explore the potential of this strategy to manipulate DNA delivery efficiency towards specific cell targets, the construction of carbohydrate-coated paCD:pDNA mixed nanoparticles (glycoCDplexes, Fig. 1, right), the evaluation of their ability to bind to carbohydrate-specific protein receptors (lectins) and the implications of glycoCDplex-lectin recognition phenomena in transfection efficiency has now been investigated. We have focused on mannosylated vectors, keeping in mind that, mannosylated pDNA-condensing materials have been claimed to promote preferential delivery to macrophages and non-parenchymal liver cells through specific interactions with the fucose-mannose receptor overexpressed at the cell surface of these cell lines [26], [27], [28] and [29].

2. Materials and methods

2.1. Synthesis

2.1.1. General methods

Reagents and solvents were purchased from commercial sources and used without further purification, with the exception of DCM, that was distilled under N2 stream over CaH2. Optical rotations were measured at 20 °C in 1-dm tubes on a Perkin–Elmer 141 MC polarimeter. IR spectra were recorded on an FTIR spectrometer. 1H (and 13C NMR) spectra were recorded at 500 (125.7), 400 (100.6), and 300 (75.5) MHz. 2D COSY, 1D TOCSY, and HMQC experiments were used to assist on NMR assignments. Thin-layer chromatography (TLC) was carried out on aluminium sheets coated with Kieselgel 30 F245 (E. Merck), with visualization by UV light and by charring with 10% H2SO4 or 0.1% ninhydrin in EtOH. Column chromatography was carried out on Silica Gel 60 (E. Merck, 230–400 mesh). Electrospray mass spectra (ESI-MS) were obtained with a Bruker Esquire6000 instrument. The starting materials heptakis[6-(2-aminoethylthio)-6-deoxy-2,3-di-O-hexanoyl]-cyclomaltoheptaose heptahydrochloride (5) [21], heptakis[6-isothiocyanato-6-deoxy-2,3-di-O-hexanoyl]cyclomaltoheptaose (6) [21], 2-isothiocyanatoethyl α-d-mannopyranoside [30], 1,6-hexamethylenediisothiocyanate [31], bis(2-aminoethyl)-[2-(tert-butoxycarbonylamino)ethyl]amine [32], N-tritylethylene-1,2-diamine [33], and 6-azido-6-deoxy-N-(2,2-diethoxycarbonylvinyl)-β-d-glucopyranosylamine [34] were prepared as described previously. Full experimental synthetic details are given as Supporting Data.

2.1.2. Synthesis of GaCD 2

A solution of 5 (85 mg, 26.9 μmol) in acetone-H2O (2:1, 3 mL) at pH 8 (NaHCO3) was stirred for 20 min and then, a solution of 2-isothiocyanatoethyl α-d-mannopyranoside [30] (75 mg, 0.28 mmol, 1.5 eq) in H2O (1 mL) was added. After 2 h, a precipitate appeared which was dissolved in DCM (0.5 mL) and the resulting solution was further stirred for 16 h. The organic solvents were concentrated and the aqueous phase was extracted with DCM, dried (Na2SO4), filtered and concentrated. The resulting residue was purified by column chromatography (1:1 → 1:2 DCM-MeOH). Yield: 49 mg (38%); [α]D = +75.1 (c 1.0 in CHCl3); 1H NMR (500 MHz, 9:1 MeOD-CDCl3, 323 K): δ = 5.32 (t, 7 H, J2,3 = J3,4 = 9.0 Hz, H-3) 5.14 (d, 7 H, J1,2 = 3.8 Hz, H-1), 4.83 (m,

14 H, H-2, H-1Man), 4.19 (m, 7 H, H-5), 3.91–3.81 (m, 28 H, H-4, H-2Man, H-6aMan, OCHa), 3.79–3.68 (m, 28 H, H-3Man, H-6bMan, CH2NCyst), 3.66 (m, 7 H, OCHb), 3.64 (t, 7 H, J3,4 = J4,5 = 9.4 Hz, H-4Man), 3.58 (m, 7 H, H-5Man), 3.30 (m, 14 H, CH2NH), 3.27 (m, 7 H, H-6a), 3.18 (m, 7 H, H-6b), 2.94, 2.89 (2 dt, 14 H, 2JH,H = 13.8 Hz, 3JH,H = 7.2 Hz, CH2SCyst), 2.45, 2.20 (m, 28 H, CH2CO), 1.62 (m, 28 H, CH2CH2CO), 1.39–1.30 (m, 56 H, CH2CH3, CH2CH2CH3), 0.92 (m, 42 H, CH3); 13C NMR (125.7 MHz, 9:1 MeOD-CDCl3, 323 K): δ = 183.8 (CS), 174.9, 173.4 (CO), 101.8 (C-1Man), 98.2 (C-1), 80.2 (C-4), 74.7 (C-5Man), 73.1 (C-5), 72.7 (C-3Man), 72.1 (C-2, C-2Man), 71.8 (C-3), 68.9 (C-4Man), 67.5 (OCH2), 63.1 (C-6Man), 45.4, 45.2 (CH2NH, CH2NCyst), 35.3 (CH2CO), 34.2 (CH2SCyst), 32.7, 32.5 (CH3CH2CH2), 30.7 (C-6), 25.6 (CH2CH2CO), 23.5 (CH3CH2), 14.6 (CH3); MALDI-TOF-MS: m/z 4723.45 [M + H]+; elemental analysis calcd (%) for C203H350N14O84S14: C 51.01, H 7.38, N 4.10; found: C 51.03, H 7.50, N 3.97.

2.1.3. Synthesis of pGaCD 3

To a solution of 5 (36 mg, 12.3 µmol) and Et3N (13 µL, 95 µmol, 1.1 eq) in DMF (1 mL), a solution of 12 (74 mg, 103 µmol, 1.2 eq) in DMF (1 mL) was added. The reaction mixture was stirred at 40 °C for 48 h. The solvent was evaporated under reduced pressure. The residue was purified by GPC (Sephadex LH-20 in MeOH) to yield compound 13 in 84% yield. Treatment of the heptacarbamate 13 (38 mg, 4.8 µmol) with 1:1 TFA-DCM (1.5 mL) at RT for 3 h, followed by evaporation of the solvent and freeze-drying from diluted HCl gave 3 (34 mg) in quantitative yield. [α]D = +29.0 (c 0.2 in MeOH); 1H NMR (500 MHz, 5:1 MeOD-D2O, 323 K): δ = 5.33 (bs, 7 H, H-3), 5.19 (bs, 7 H, H-1), 4.87 (bs, 7 H, H-1Man), 4.85 (bs, 7 H, H-2), 4.19 (bs, 7 H, H-5), 4.03 (bs, 28 H, H-4, CH2NH2), 3.94 (m, 7 H, H-2Man), 3.87 (m, 21 H, H-6aMan, CH2Oa), 3.75 (m, 70 H, H-3Man, H-6bMan, CH2CH2S, CH2NHCS, CH2Ob, H-4Man), (14 H, NCH2), 3.58 (m, 45 H, H-5Man, CH2CH2O, CH2CH2NH2), 3.46 (m, 28 H, CH2NHCS), 3.30 (m, 7 H, H-6a), 3.17 (m, 7 H, H-6b), 2.94 (m, 14 H, CH2SCyst), 2.50–2.20 (m, 28 H, CH2CO), 1.63 (m, 56 H, CH2CH2CO, CH2CH2NHCS), 1.38 (m, 84 H, CH2CH3, CH2CH2CH3, CH2CH2CH2NHCS), 0.94 (m, 42 H, CH3); 13C NMR (125.7 MHz, MeOD, 323 K): δ = 183.0–181.0 (CS), 174.0–171.0 (CO ester), 100.2 (C-1Man), 96.9 (C-1), 79.0 (C-4), 75.0 (C-5), 73.2 (C-5Man), 71.1 (C-3Man), 70.6 (C-2Man), 70.5 (C-3), 67.2 (C-4Man, C-2), 65.9 (CH2O), 61.3 (C-6Man), 54.6 (CH2CH2NHCSTren), 50.7 (CH2CH2NH2), 44.4–44.0 (CH2NHCSsp, CH2CH2SCyst, CH2NHCSTren), 39.2 (CH2NH2), 34.4 (CH2CH2O), 33.8 (CH2CO, C-6), 33.0 (CH2SCyst), 31.2 (CH2CH2CH3), 28.6 (CH2CH2NHCSsp), 26.4 (CH2CH2CH2NHCS), 24.3, 24.2 (CH2CH2CO), 22.2 (CH2CH3), 13.5, 13.3 (CH3); ESI-MS: m/z 2401.2 [M + 3 H]3+, 1801.4 [M + 4 H]4+, 1442.1 [M + 5 H]5+; elemental analysis calcd (%) for C301H567Cl7N56O84S28: C 48.45, H 7.66, N 10.51; found: C 48.25, H 7.426, N 10.29.

2.1.4. Synthesis of pGaCD 4

To a solution of 21 (40 mg, 105 µmol) in DMF (2 mL) and Et3N (14 µL, 0.1 mmol, 1.1 eq) was added a solution of 6 (44 mg, 13.6 µmol) in DCM (1 mL) and the reaction mixture was stirred at RT for 7 days. The solvent was removed under vacuum and the residue purified by column chromatography (70:10:1 DCM-MeOH-H2O) to furnish compound 22 in 76% yield. Heptacarbamate 22 was then treated with mixture of TFA-DCM (1:1, 2 mL) at RT for 2 h. Then solvent was evaporated and acid traces were removed by co-evaporation with water, and the residue was freeze-dried from diluted HCl to afford 4 (99% yield). [α]D = +426.5 (c 0.75 in MeOH); 1H NMR (500 MHz, 5:1 MeOD-D2O, 333 K): δ = 5.40 (m, 7 H, H-1Glc), 5.33 (t, 7 H, J2,3 = J3,4 = 9.0 Hz, H-3), 5.19 (d, 7 H, J1,2 = 3.6 Hz, H-1), 4.86 (dd, 7 H, J1,2 = 4.0 Hz, H-2), 4.20 (m, 7 H, H-5), 3.94 (t, 7 H, J4,5 = 9.0 Hz, H-4), 3.70 (m, 7 H, H-5Glc), 3.74 (bs, 42 H, 2 CH2NHCS, CH2NCyst), 3.56 (t, 7 H, J2,3 = J3,4 = 9.0 Hz, H-3Glc), 3.51 (m, 7 H, H-2Glc), 3.46 (ddd, 7 H, J6a,6b = 14 Hz, J5,6a = 2.8 Hz, H-6aGlc), 3.31 (m, 7 H, H-4Glc), 3.18 (m, 14 H, H-6a, H6b), 3.09

(dd, 7 H, J5,6b = 8.8 Hz, H-6aGlc), 2.97 (bs, 14 H, CH2SCys), 2.45–2.28 (m, 28 H, CH2CO), 1.66 (m, 28 H, CH2CH2CO), 1.37 (m, 56 H, CH2CH3, CH2CH2CH3), 0.95 (m, 42 H, CH3); 13C NMR (125.7 MHz, DMSO-d6, 323 K): δ = 186.4, 185,7 (CS), 175.6, 174.5 (C-1Hex), 99.3 (C-1), 86.5 (C-1Glc), 80.1 (C-4), 75.4 (C-3Glc) 74.5 (C-5Glc), 74.6 (C-6, C-2Glc,C-4Glc), 74.2 (C-5), 73.3 (C-2, C-3), 46.8, 46.5, 46.1 (CH2NHCS), 36.5, 36.4 (CH2CO), 35.7 (CH2NCyst), 33.9, 33.8 (CH2CH2CH3), 32.0 (C-6Glc), 27.0, 26.9 (CH2CH2CO), 24.9 (CH2CH3), 16.7 (CH3); ESI-MS: m/z 1727.1 [M + 3 H]3+; elemental analysis calcd (%) C210H378N35O70S21: C, 46.41; H, 7.01; N, 9.02; found: C, 46.29; H, 6.88; N, 8.87.

2.2. Preparation and characterization of CDplexes

2.2.1. Preparation of nanocomplexes composed of CD derivatives and plasmid pTG11236

The plasmid pTG11236 (pCMV-SV40-luciferase-SV40 pA), used for the preparation of the pDNA complexes and for transfection assay is a plasmid of 5739 bp (base pairs). The quantities of compound used were calculated according to the desired DNA concentration of 0.1 mg mL−1 (303 µm phosphate), the N/P ratio, the molar weight and the number of protonable nitrogens in the selected CD derivative or JetPEI [35] and [36]. Experiments were performed for N/P 5 and 10. Concerning the preparation of the DNA complexes from CD derivatives and JetPEI, pDNA was diluted in HEPES (20 mm, pH 7.4) to a final concentration of 303 µm, and then the desired amount of CD derivative was added from 10 or 20 mm stock solution (DMSO). For JetPEI polyplexes, pDNA was diluted in a 150 mm NaCl solution to a final phosphate concentration of 303 µm, and then the desired amount of JetPEI was added from a 7.5 mm water solution. The preparation was vortexed for 2 h and used for characterization or transfection experiments.

2.2.2. Agarose gel electrophoresis

Each CD derivative/DNA formulation (20 µL, 0.4 µg of plasmid) was submitted to electrophoresis for about 30 min under 150 V through a 0.8% agarose gel in TAE 1X (Tris-acetate-EDTA) buffer and stained by spreading an ethidium bromide (Sigma) solution in TAE buffer (20 µL ethidium bromide of a 10 mg mL−1 solution in 200 mL TAE). The DNA was then visualized after photographing on an UV transilluminator. The plasmid integrity in each sample was confirmed by electrophoresis after decomplexation with sodium dodecyl sulfate (SDS, 8%).

2.2.3. Measurement of the size of the complexes by dynamic light scattering (DLS) and of the zeta potential

The average sizes of the glycoCDplexes were measured using a Zetasizer nano (Malvern Instruments, Paris, France) with the following specification: sampling time, automatic; number of measurements, 3 per sample; medium viscosity, 1.054 cP; refractive index, 1.33; scattering angle, 173°; λ = 633 nm; temperature, 25 °C. Data were analyzed using the multimodal number distribution software included in the instrument. Results are given as volume distribution of the major population by the mean diameter with its standard deviation. Zeta potentials measurements on the glycoCDplexes were made with the same apparatus using “Mixed Mode Measurement” phase analysis light scattering.

2.2.4. “Mixed Mode Measurement” phase analysis light scattering (M3-PALS)

M3 consists of both slow field reversal and fast field reversal measurements, hence the name ’Mixed Mode Measurement’ that improves accuracy and resolution. The following

specifications were applied: sampling time, automatic; number of measurements, 3 per sample; medium viscosity, 1.054 cP; medium dielectric constant, 80; temperature, 25 °C.

Before each series of experiment, the performance of the instruments was checked with either a 90 nm monodisperse latex beads (Coulter) for DLS or with DTS 50 standard solution (Malvern) for zeta potentials.

2.2.5. Transmission electron microscopy (TEM)

Formvar-carbon coated grids previously made hydrophilic by glow discharge were placed on top of small drops of the CDplex samples (Hepes 20 mm, pH 7.4, DNA 303 µm phosphate) prepared as described above. After 1–3 min of contact, grids were negatively stained with a few drops of 1% aqueous solution of uranyl acetate. The grids were then dried and observed with a Philips CM12 electron microscope working under standard conditions. All these experiments were reproduced twice on each formulation.

2.3. Determination of mannose-specific receptor binding capabilities of CDplexes

2.3.1. Inhibition of concanavalin A (Con A)–immobilized mannan binding by enzyme-linked lectin assay (ELLA)

Nunc-Inmuno™ plates (MaxiSorp™) were coated overnight with yeast mannan at 100 µL/well diluted from a stock solution of 10 µg mL−1 in 10 mm phosphate buffer saline (PBS, pH 7.3 containing 0.1 mm Ca2+ and 0.1 mm Mn2+) at room temperature. The wells were then washed three times with 300 µL of washing buffer (containing 0.05% (v/v) Tween 20) (PBST). The washing procedure was repeated after each of the incubations throughout the assay. The wells were then blocked with 150 µL/well of 1% BSA/PBS for 1 h at 37 °C. After washing, the wells were filled with 50 µL of 20 mm HEPES buffer (pH 7.4) and 50 µL of serial dilutions of horseradish peroxidase labelled concanavalin A (Con A-HRP, Sigma) from 10−1 to 10−4 mg mL−1 in PBS, and incubated at 37 °C for 1 h. The plates were washed and 50 µL/well of 2,2′-azinobis-(3-ethylbenzothiazoline-6-sulfonic acid) diammonium salt (ABTS) (0.25 mg mL−1) in citrate buffer (0.2 m, pH 4.0 with 0.015% H2O2) was added. The reaction was stopped after 20 min by adding 50 µL/well of 1 m H2SO4 and the absorbances were measured at 415 nm. Blank wells contained citrate-phosphate buffer. The concentration of lectin-enzyme conjugate that displayed an absorbance between 0.8 and 1.0 was used for inhibition experiments.

In order to carry out the competitive lectin binding inhibition experiments, each paCD or paCD-pDNA nanocomplex was added in a serial of 2-fold dilutions (60 µL per well) in HEPES buffer to 60 µL of the appropriate Con A-HRP concentration in PBS buffer on Nunclon™ (Delta) microtitre plates and incubated for 1 h at 37 °C. The above solutions (100 µL) were then transferred to the mannan-coated microplates, which were incubated for 1 h at 37 °C. The plates were washed and the ABTS substrate was added (50 µL per well). Color development was stopped after 20 min and the absorbances were measured. The percent of inhibition was calculated as follows:

$$\text{Inhibition}(\%) = 100 \times \left(A_{(\text{no inhibitor})} - A_{(\text{with inhibitor})}\right) / A_{(\text{no inhibitor})}$$

IC50 values (concentration required for 50% inhibition of the lectin–immobilized yeast mannan association) were calculated relative to that reported for methyl α-d-mannopyranoside (865 µm) [37]. Typically, the IC50 values obtained from several independently performed tests were highly reproducible.

2.3.2. Inhibition of macrophage mannose receptor (MMR)–immobilized mannan binding by ELLA

The inhibition experiment designed for determining the relative binding potency of CD:pDNA nanocomplexes to the human macrophage mannose receptor has been adapted from the method reported by Euzen and Reymond for Con A [38]. 96-Well titreplates were coated with yeast mannan and blocked with BSA as described above for Con A binding assays. The wells were filled with 100 µL of serial dilutions of recombinant human macrophage mannose receptor (rhMMR) from a 10 µg mL−1 stock solution in PBS (pH 7.3 containing 0.1 mm Ca2+ and 0.1 mm Mn2+), and incubated at 37 °C for 1 h. The plates were washed three times with PBST as described above and 100 µL of a solution of biotinylated Anti-human MMR antibody (0.2 µg mL−1, R&D Systems) in PBS was added in each well, and the plates were further incubated for 1 h at 37 °C. The complex NeutrAvidin®–biotinylated HRP was preformed separately by successively adding to Tris buffer (9.6 mL, 50 mm, pH 7.6) a solution of Neutravidin® (100 µg mL−1 in Tris buffer, 1.2 mL, Thermo Scientific) and a solution of biotin-conjugated HRP (25 µg mL−1 in Tris buffer, 1.2 mL, Thermo Scientific). The mixture was shaken for 30 min at rt and the solution was immediately transferred into the plates (60 µL per well). After 1 h at 37 °C, these plates were washed twice with Tris (250 µL per well) and 2,2′-azinobis-(3-ethylbenzothiazoline-6-sulfonic acid) diammonium salt (ABTS, 0.25 mg mL−1, 50 mL per well) in citrate buffer (0.2 m, pH 4.0 with 0.015% H2O2) was added. After 5 min at room temperature, the optical density at 415 nm was measured. Blank wells were processed with Anti-human MMR antibody as well as NeutrAvidin®-biotinylated HRP. The concentration of rhMMR that displayed an absorbance between 0.8 and 1.0 was used for inhibition experiments.

In order to carry out the competitive lectin binding inhibition experiments, each paCD or paCD-pDNA nanocomplex was mixed in a serial of 2-fold dilutions (60 mL per well) in HEPES buffer (20 mm, pH 7.4) with 60 µL of the appropriate rhMMR concentration in PBS buffer on Nunclon™ (Delta) microtitre plates and incubated for 1 h at 37 °C. The above solutions (100 µL) were then transferred to the mannan-coated titreplates, which were incubated for 1 h at 37 °C. The plates were washed and the solution of biotinylated Anti-human MMR antibody in PBS (100 µL) was added in each well, and the plates were further incubated for 1 h at 37 °C. Then the NeutrAvidin solution was transferred into the plates (60 mL per well). After 1 h at 37 °C, these plates were washed twice with Tris (250 µL per well) and ABTS was added (50 mL per well). Optical density at 415 nm was determined at 5 min. The percentage of inhibition was calculated as described above for classical ELLA.

2.3.3. Macrophage adhesion assays

For evaluation of the interaction of YOYO-1-labeled CDplexes with macrophages, the procedure reported by Muller and Schuber [39] for mannosylated liposomes was adapted. Briefly, resident peritoneal macrophages were obtained from female Balb/c mice (6–8 weeks old) and maintained in Dulbecco's modified Eagle's medium (DMEM) supplemented with 10% decomplemented fetal calf serum (FCS) containing heparin (5 U/mL). The cell number was adjusted to 106 cells/mL and the suspension was platted (final volume 1 mL) in multi-well plates. After 2 h in a humidified atmosphere of 5% CO2 in air (final pH 7.4), non-adherent cells were eliminated by rinsing the dishes three times with PBS. The adherent cells, 24 h after their isolation, were fed with fresh serum-less DMEM and incubated with varying amounts of CD-pDNA nanocomplexes, PEI polyplexes and naked DNA (control). After the incubation time, the medium was pipetted-off and the cells washed four times with cold PBS (4 °C). The fluorescent

tag associated to the cells was measured fluorimetrically (Perkin-Elmer luminescence spectrometer LS50B, excitation at 491 nm and monitoring emission at 509 nm) after cell digestion in 1 mL PBS containing 0.1% of emulphogene BC-720, and scraping with a rubber policeman. Experiments were run in duplicate, and results did not differ more than 10%.

2.4. Cell-based assays

2.4.1. In vitro transfection

Twenty-four hours before transfection, BNL-CL2 or RAW 264.7 cells were grown at a density of 2 × 104 cells/well in a 96-well plates in Dulbelco modified Eagle culture medium (DMEM; Gibco-BRL) containing 10% foetal calf serum (FCS; Sigma) and 10 mg/mL gentamycin for BNL-CL2 cells, or in RPMI 1640 (Gibco-BRL) containing 10% FCS, 100 units/mg penicillin and 100 µg/mL streptomycin for RAW 264.7 cells, in a wet (37 °C) and 5% CO2/95% air atmosphere. The above described CD:pDNA complexes and JetPEI:pDNA polyplexes were diluted to 100 µL in DMEM or in DMEM supplemented with 10% FCS, with or without yeast mannan (5 mg mL−1), in order to have 0.5 µg of pDNA in the well (15 µm phosphate). The culture medium was removed and replaced by these 100 µL of complexes. After 4 h and 24 h, 50 and 100 µL of DMEM supplemented with 30% and 10% FCS, respectively, were added. After 48 h, the transfection was stopped, the culture medium was discarded, and the cells washed twice with 100 µL of PBS and lysed with 50 µL of lysis buffer (Promega, Charbonnières, France). The lysates were frozen at −32 °C, before the analysis of luciferase activity. This measurement was performed in a luminometer (GENIOS PRO, Tecan France S.A) in dynamic mode, for 10 s on 20 µL on the lysis mixture and using the “luciferase” determination system (Promega) in 96-well plates. The total protein concentration per well was determined by the BCA test (Pierce, Montluçon, France). Luciferase activity was calculated as femtograms (fg) of luciferase per mg of protein. The percentage of cell viability was calculated as the ratio of the total protein amount per well of the transfected cells relative to that measured for untreated cells × 100. The data were calculated from three or four repetitions in two fully independent experiments (formulation and transfection).

2.4.2. Statistical analysis

Statistical tests were performed with STATGRAPHICS Plus 5.0 software. Analysis of variance (Anova) was run on the logarithmic transformation of transfection levels (Log10[fg luciferase/mg protein]) and on the cell viability to fit normal distributions of the data. Two factors, i.e. nature of the complexing agent (CD derivative and JetPEI) and N/P ratio, were analysed as source of the variation of logarithmic transformation of the transfection levels and of cell variability percentages using a multiple comparison procedure. The Tukey’s honestly significant difference (HSD) method was used to discriminate among the means of cell viability percentages and the logarithmic transformation of luciferase expression levels.

2.4.3. Flow cytometry (fluorescence assisted cell sorting, FACS)

For flow cytometry experiments, the plasmid DNA was first labelled with YOYO (Molecular Probes, Eugene, USA) at a 1 YOYO per 150 base pairs (i.e. 38 molecules/plasmid) prior to its condensation with the CDs or JetPEI at an N/P ratio of 10, as described above. 125 µL of these DNA complex dispersions were diluted to 500 µL in serum-free DMEM, without or with yeast mannan (5 mg mL−1), in order to have 2.5 µg of DNA in the well (DNA concentration of 15 mM phosphate). Twenty-four hours before cell uptake experiments, RAW 264.7 or BNL-CL2 cells were seeded at a density of 1 × 105 cells/well in 24-well plates into RPMI 1640 supplemented

with 10% FCS, 100 units/mg penicillin, 100 µg/mL streptomycin (for RAW 264.7 cells) or into DMEM supplemented with 10% FCS and 10 mg/mL gentamycin (for BNL-CL2 cells) at 37 °C in a 5% CO2 humidified atmosphere for 24 h. The culture medium was removed and replaced by 500 µL of the respective YOYO-labelled DNA complexes. After 4 h of incubation at 37 °C, the culture medium was discarded, and cells were incubated for 15 min at 37 °C in a 5% CO2 humidified atmosphere with 1 mL of a 200 mg/L calf thymus solution into DMEM (serum free) to remove unspecific binding. Cells were then washed twice with 200 µL of cold PBS then harvested by trypsination, resuspended in 500 µL of DMEM with 10% of FCS, collected by centrifugation (5 min, 2000 rpm), washed twice with 500 µL of cold PBS, and then resuspended in PBS/1% EDTA. Flow cytometry analysis was performed with a FACS Calibur (BD Biosciences) using an argon laser (excitation at 488 nm for YOYO). Sorting windows were used on forward and side scatter to eliminate debris. Granulation, size and fluorescence intensity (emission 515 nm for YOYO) were recorded at a rate of 300 cells/s. Data were analyzed using winMDI 2.8 version software. For the experiments performed at 4 °C, the same protocol was applied except that the cells, after seeding at 37 °C, were first cooled to this temperature before the culture medium was removed and replaced by the respective YOYO-labelled DNA complex solution also cooled to 4 °C, then incubated at 4 °C for 4 h.

3. Results and discussion

3.1. Synthesis of pGaCDs and characterization of self-assembling capabilities

In a first approach, pDNA complexation by mixtures of paCD 1[20] and [21] and the neutral glyco-amphiphilic cyclodextrin (GaCD) 2, bearing a heptavalent α-d-mannopyranosyl cluster, was attempted. Disappointingly, the resulting nanoparticles failed to fully protect pDNA from the environment and mediate gene transfection even at low proportions (5–10%) of 2.

This negative result was ascribed to a mismatching effect of segregated polycationic and neutral microdomains at the nanoparticle surface and/or core upon interaction with pDNA, leading to disruption of the three-component supramolecular assemblies. To overcome this problem, two different prototypes of polycationic glyco-amphiphilic CDs (pGaCDs) displaying regular arrangements of glyco-cationic moieties, namely compounds 3 and 4 (Fig. 2), were designed. In the case of 3, α-d-mannopyranosyl residues share the same space region than ammonium groups in alternating branches. In pGaCD 4 the positive charges are installed at the primary O-6 position of β-d-glucopyranosyl units, featuring a multivalent architecture that was inspired on that of aminoglycoside antibiotic-based cationic lipids. The 6-aminoglucosyl moiety in such systems has been shown to be well-suited to interact with double-stranded DNA [40], but is not a ligand for cell surface lectins. It would then serve as negative control for targeting evaluation.

The preparation of pGaCDs 3 and 4 followed convergent synthetic schemes in which the key step is the coupling reaction of βCD heptaamine 5[21] or heptaisothiocyanate 6[21] with complementary isothiocyanate- or amine-armed glycoconjugates (Scheme 1 and Scheme 2). The synthesis of the heterobifunctional antenna in pGaCD 3 started from the orthogonally protected branching element 7, which was reacted with the per-O-acetylated 2-isothiocyanatoethyl-α-d-mannopyranoside 8 to furnish the thiourea adduct 9 in almost quantitative yield (Scheme 1). Sequential acetyl and trityl cleavage yielded amine 11 (97% over two steps), which was then reacted with an excess of 1,6-hexamethylenediisothiocyanate [31] (→12, 52%). Et3N-catalysed thiourea-forming reaction between 12 and heptamine 5 in DMF at

40 °C afforded the Boc-protected βCD heptaconjugate 13 in a more than satisfactory 84% yield. Final carbamate cleavage furnished the target pGaCD 3 in quantitative yield.

The synthesis of pGaCD 4 required isothiocyanate 18 as the aminoglucosyl coating reagent. Its synthesis started from the known 6-azidoglucosylenamine 14[41] (Scheme 2). Reduction of the azido group with 1,3-propanedithiol [42] and [43] and protection of the resulting amine 15 as the corresponding Boc derivative furnished carbamate 16. Further O-acetylation (→17), enamine chlorolysis and isothiocyanation with thiophosgene afforded isothiocyanate 18 in 54% overall yield. Compound 18 was first coupled with N-tritylethylene-1,2-diamine, followed by sequential acetyl and trityl cleavage to yield amine 21 (73% over two steps). Nucleophilic addition of 21 to heptaisothiocyanate 6 in a mixture of DCM-DMF proceeded smoothly at room temperature to furnish the fully substituted βCD adduct 22, which was finally subjected to acid-catalyzed carbamate hydrolysis to yield the target heptavalent aminoglycocluster 4 (75% overall).

The NMR, ESI-MS and combustion analysis data for 3 and 4 were consistent with the expected C7-symmetric arrangement for homogeneously substituted βCD derivatives, attesting for the efficiency of the proposed synthetic scheme to control vector topology. Both 3 and 4 self-assembled in the presence of pDNA to form stable cationic glycoCDplexes at protonable nitrogen/phosphorous (N/P) ratio ≥5 that fully protected pDNA from the environment, as seen from gel electrophoresis retardation and accessibility experiments using the intercalating agent ethidium bromide. Dynamic light scattering (DLS) afforded average diameters of 80 ± 35 and 100 ± 20 nm, with ζ potentials of +40 ± 1 and +48 ± 1 mV for the 3:pDNA and 4:pDNA nanocondensates at N/P 10, respectively (Table 1). Transmission electron microscopy (TEM) confirmed the small size and homogeneous distribution of the glycoCDplexes (Fig. 3). Image magnification evidenced a snake-like ultrastructure probably arising from alternating packing of electron-dense (pDNA strains) and electron-deficient (lamellar pGaCD arrangements) regions [21] and [40].

3.2. Mannose-specific receptor binding capabilities of glycoCDplexes

The ability of the 3:pDNA nanoparticles to interact with mannose-specific lectins was first evaluated by measuring the inhibition of binding between immobilized mannan and concanavalin A (ConA) lectin by enzyme-linked lectin assay (ELLA) [38] and [44]. The data were indicative of a strong affinity (IC50 22 μm), in agreement with the presence of a high-valency display of mannopyranosyl residues at the surface of the CDplexes [45]. In contrast, the glucose-coated nanoparticles 4:pDNA did not exhibit any significant binding capabilities towards this lectin (Fig. 4).

Because lectins having identical sugar binding motifs may differ significantly in their binding site, quaternary structure, and preferred binding mechanisms, the conclusions obtained for a particular receptor, for example, the plant lectin ConA in the present study, must be taken with care when changing the lectin target. To test the potential of the mannosylated 3:pDNA nanoparticles in drug targeting, assaying a human lectin was, therefore, of interest. For this purpose, the ELLA protocol was adapted to the inhibition of binding of the soluble human macrophage mannose receptor (MMR; recombinant protein product commercially available from R&D systems, Catalogue Number: 2534 MR) to immobilized yeast mannan (see supporting information for details). The results unequivocally demonstrated that 3:pDNA glycoCDplexes are also recognized by the human MMR and that the nanoparticle-MMR interaction is specific for DNA complexes exposing mannosyl ligands (Fig. 4).

MMR-mediated endocytosis of glycoCDplexes in intact macrophages might compete with non-specific internalization following electrostatic interactions with cell-surface proteoglycans (i.e., both internalization routes depicted in Fig. 1) [46]. To evaluate the relative weight of these two mechanisms, adhesion of the nanoparticles to resident peritoneal macrophages (mice) was studied. Binding of the targeted glycoCDplexes and the controls (1:pDNA and 4:pDNA nanocondensates) were quantified by a fluorimetric method reported for mannosylated liposomes [39] using YOYO-labelled DNA. Neutral mannosylated cyclodextrins had been shown previously to be recognized and specifically internalized under these experimental settings [32]. Polyplexes prepared from polyethyleneimine (PEI, 25 kDa) were included in this study as an additional reference. Experiments were performed at 4 °C, a temperature that precludes phagocytosis, for CDplex concentrations and conditions identical to those used during transfection experiments. As illustrated in Fig. 5, the fluorimetric assay clearly demonstrated a much higher level of cell labeling with 3:pDNA as compared with 1:pDNA or 4:pDNA. At N/P 10, however, the fraction of CDplexes binding to the macrophage surface through MMR-independent interactions increased very significantly (Fig. 5A). To define the specificity of the interaction, competition experiments using mannosylated bovine serum albumin (ManBSA) were carried out at N/P 5 (Fig. 5B). The results were consistent with reversible binding of the mannosylated nanoparticles 3:pDNA to the cell surface, competing for the same binding site as ManBSA. In contrast, when 1:pDNA or 4:pDNA CDplexes were used, no direct competition was observed. Control experiments using BSA strongly supports the involvement of MMR in the former case.

3.3. Cell uptake and transfection efficiency of glycoCDplexes

In the light of the above results, further transfection experiments using a luciferase-encoding reporter gene were monitored for nanoparticles formulated at N/P 5 in RAW 264.7 (mouse leukaemic monocyte macrophage cells), known to express moderate mannose receptors involved in receptor-mediated endocytosis at the cytoplasmic membrane [47]. Transfection using 3:pDNA CDplexes in RAW 264.7 cells proved to be about 100-fold more efficient as compared with CDplexes prepared from the isoelectronic pGaCD derivative 4 (Fig. 6). The transfection efficiency was actually comparable to that achieved with nanoparticles prepared from the non-glycosylated paCD 1, bearing double number of protonable amino groups, but with a much more favorable toxicity profile (92 versus 46% cell viability). The fact that transfection efficiency dropped down to basal values in the presence of yeast mannan (5 mg mL−1) for 3:pDNA nanoparticles but remained unaltered for 1:pDNA or 4:pDNA CDplexes strongly points at the involvement of MMR in the uptake of the mannosylated material.

The above end was further supported by fluorescence activated cell sorting (FACS) experiments using YOYO-labelled nanoparticles. No cell uptake occurred with any of the coated or un-coated CDplexes when the experiments were conducted at 4 °C. When the experiments were conducted at 37 °C, internalization of the mannosylated 3:pDNA CDplexes in RAW 264.7 cells was substantially inhibited in the presence of yeast mannan (Fig. 7), suggesting that MMR-dependent uptake is the most relevant mechanism operating in this case. Such an inhibition was not observed in the case of BNL-CL2 (murine hepatocytes) cells (data not shown). Parallel FACS experiments with nanoparticles prepared from 1, 4 or the polycationic polymer JetPEI as controls confirmed that internalization was MMR-independent for mannose-devoid systems (see Supplementary Data).

To assess the potential of 3:pDNA nanoparticles as site-specific gene delivery systems, further transfection experiments were carried out towards BNL-CL2 cells that do not express mannose

receptors. At N/P 5, 3:pDNA nanoparticles were unable to produce any significant increase in gene expression in this cell line as compared to naked DNA (Fig. 8). By comparison, CDplexes obtained from the non-glycosylated paCD 1 transfected these cells with a 10-fold higher efficiency than RAW 264.7 cells (up to 103-folds relative to naked pDNA in BNL-CL2 cells as compared to 102-folds in RAW 264.7 cells). The presence of the mannopyranosyl substituents at the 3:pDNA nanocomplexes probably shields the positively charged amino centers at the nanocomplex surface, weakening electrostatic interactions with cell membrane proteoglycans and limiting internalization through non-specific routes. Actually, nanoparticles obtained from the control aminoglucosyl pGaCD 4 at N/P 5 exhibited a very low transfection profile in all cell lines assayed, irrespective of the presence or not of mannose-specific receptors.

It should be stressed that a proper balance between the biorecognition and shielding roles of the sugar moieties at the surface of the nanocomplexes is critical for cell-specific targeting and must be carefully considered when formulating pGaCD:pDNA nanoparticles. Non-glycosylated paCD:pDNA CDplexes (e.g. those prepared from 1) behave as broad-range gene delivery systems, with efficiency profiles that challenge and even overpass that of the polycationic polymer JetPEI, one of the most popular commercially available nonviral gene vectors [35] and [36]. CDplexes obtained from pGaCDs 3 and 4 likewise transfected the two cell lines used in this study with enhanced efficiency at N/P 10, but with low selectivity (data not shown). At N/P 5, however, receptor-mediated internalization mechanisms are favored and site-specific gene delivery becomes feasible.

4. Conclusions

Targeting involving sugar binding to biological receptors has generally relied on the generation of large multivalent displays of the putative epitopes onto nanometric carriers. Our results show that it is possible to attain biologically useful affinities by using molecular polycationic glycoclusters of appropriate topology that can undergo self-assembling in the presence of nucleic acids, thereby generating glyco-coated nanoparticles. Synthetic methods that allow not only the efficient coupling of the sugar moieties but also the installation of the relevant functional elements with a precise spatial orientation onto a cyclodextrin core can be exploited to tailor the pDNA-pGaCD association and the nanocomplex–lectin interactions. The approach is purposely conceived to be compatible with molecular diversity-oriented strategies and should facilitate exploration of structural modifications on the hierarchical process going from individual pGaCDs to self-assembled CDplexes to CDplex:lectin complexes. In this context, the significance of the present study is three-fold. First, it demonstrates an efficient and very flexible strategy for the preparation of tailor-made pGaCDs bearing biorecognizable markers or reporting groups. Second, it has been shown that monodisperse pGaCDs are able to compact pDNA to form small nanoparticles in which the genetic material is fully protected from the environment. Third, the present system suggests a potential utility in sugar-directed delivery of gene drugs to specific saccharide-recepting biological surfaces.

Acknowledgement

This work was supported by the Spanish Ministerio de Innovación y Ciencia (MICINN, contract numbers SAF2010-15670, and CTQ2010-15848), the Junta de Andalucía (P06-FQM-01601), the European Union (FEDER and FSE), the CSIC, the CNRS and FUSINT (CNR project). A. D.-M., N. G., C. B. and A. M.-A. are grateful to the CSIC, CNRS/Région Provences, Alpes Côte d'Azur, the Ministère de l'Enseignement supérieur et de la Recherche, and the MICINN (FPU program), respectively, for pre-doctoral fellowships. We also thank the CITIUS for technical support.

References

[1] D.J. Glover, H.J. Lipps, D.A. Jans

Non-viral approaches towards safe, stable therapeutic gene expression in humans

Nat Rev Genet, 6 (2005), pp. 299–310

[2] M.A. Mintzer, E.E. Simanek

Nonviral vectors for gene delivery

Chem Rev, 109 (2009), pp. 259–302

[3] E. Wagner

Strategies to improve DNA polyplexes for in vivo gene transfer: will "artificial viruses" be the answer?

Pharmacol Res, 21 (2004), pp. 8–14

[4] T. Niidome, L. Huang

Gene therapy progress and prospects: nonviral vectors

Gene Ther, 9 (2002), pp. 1647–1652

[5] H. Akita, H. Harashima

Advances in non-viral gene delivery: using multifunctional envelope-type nano-device

Expert Opin Drug Deliv, 5 (2009), pp. 847–859

[6] B. Demeneix, Z. Hassani, J.-P. Behr

Towards multifunctional synthetic vectors

Curr Gene Ther, 4 (2004), pp. 445–455

[7] J. Sunshine, J.J. Green, K.P. Mahon, F. Yang, A.A. Eltoukhy, D.N. Nguyen et al.

Small-molecule end-groups of linear polymer determine cell-type gene-delivery efficacy

Adv Mater, 21 (2009), pp. 4947–4951

[8] E. Wagner, C. Culmsee, S. Boeckle

Targeting of polyplexes: toward synthetic virus vector systems

Adv Genet, 53 (2005), pp. 333–354

[9] H. Mok, T.G. Park

Functional polymers for targeted delivery of nucleic acid drugs

Macromol Biosci, 9 (2009), pp. 731–743

[10] J. Guo, K.A. Fisher, R. Darcy, J.F. Cryan, C. O'Driscoll

Therapeutic targeting in the silent era: advances in non-viral siRNA delivery

Mol Biosyst, 6 (2010), pp. 1143–1161

[11] M.E. Davis

The first targeted delivery of siRNA in humans via a self-assembling, cyclodextrin polymer-based nanoparticle: from concept to clinic

Mol Pharm, 6 (2009), pp. 659–668 [and references therein]

[12] C. Ortiz Mellet, J.M. Benito, J.M. García Fernández

Preorganized, macromolecular, gene-delivery systems

Chem-Eur J, 16 (2010), pp. 6728–6742

[13] V. Bagnacani, F. Sansone, G. Donofrio, L. Baldini, A. Casnati, R. Ungaro

Macrocyclic nonviral vectors: high cell transfection efficiency and low toxicity in a lower rim guanidinium calix[4]arene

Org Lett, 10 (2008), pp. 3953–3956

[14] F. Sansone, M. Dudic, G. Donofrio, C. Rivetti, L. Baldini, A. Casnati et al.

DNA condensation and cell transfection properties of guanidinium calixarenes: dependence on macrocycle lipophilicity, size, and conformation

J Am Chem Soc, 128 (2006), pp. 14528–14536

[15] C. Ortiz Mellet, J.M. García Fernández, J.M. Benito

Cyclodextrin-based gene delivery systems

Chem Soc Rev, 40 (2011), pp. 1586–1608

[16] H. Wang, K. Liu, K.-J. Chen, Y. Lu, S. Wang, W.-Y. Lin et al.

A rapid pathway toward a superb gene delivery system: programming structural and functional diversity into a supramolecular nanoparticle library

ACS Nano, 4 (2010), pp. 6235–6243

[17] H. Huang, H. Yu, G. Tang, Q. Wang, J. Li

Low molecular weight polyethylenimine cross-linked by 2-hydroxypropyl-γ-cyclodextrin coupled to peptide targeting HER2 as a gene delivery vector

Biomaterials, 31 (2010), pp. 1830–1838

[18] X. Lu, Y. Ping, J.F. Xu, Z.H. Li, Q.Q. Wang, J.H. Chen et al.

Bifunctional conjugates comprising β-cyclodextrin, polyethylenimine, and 5-fluoro-2'-deoxyuridine for drug delivery and gene transfer

Bioconjug Chem, 21 (2010), pp. 1855–1863

[19] Y. Chen, Y.-M. Zhang, Y. Liu

Multidimensional nanoarchitectures based on cyclodextrins

Chem Commun, 46 (2010), pp. 5622–5633

[20] A. Díaz-Moscoso, P. Balbuena, M. Gómez-García, C. Ortiz Mellet, J.M. Benito, L. Le Gourriérec et al.

Rational design of cationic cyclooligosaccharides as efficient gene delivery systems

Chem Commun (2008), pp. 2001–2003

[21] A. Díaz-Moscoso, L. Le Gourriérec, P. Balbuena, M. Gómez-García, J.M. Benito, N. Guilloteau et al.

Polycationic amphiphilic cyclodextrins for gene delivery: synthesis and effect of structural modifications on plasmid DNA complex stability, cytotoxicity, and gene expression

Chem-Eur J, 15 (2009), pp. 12871–12888

[22] C. Byrne, F. Sallas, D.K. Rai, J. Ogier, R. Darcy

Poly-6-cationic amphiphilic cyclodextrins designed for gene delivery

Org Biomol Chem, 7 (2009), pp. 3763–3771

[23] A. Díaz-Moscoso, D. Vercauteren, J. Rejman, J.M. Benito, C. Ortiz Mellet, S.C. De Smedt et al.

Insights in cellular uptake mechanisms of pDNA–polycationic amphiphilic cyclodextrin nanoparticles (CDplexes)

J Control Release, 143 (2010), pp. 318–325

[24] C. Biesa, C.-M. Lehra, J.F. Woodley

Lectin-mediated drug targeting: history and applications

Adv Drug Deliv Rev, 56 (2004), pp. 425–435

[25] H. Zhang, Y. Ma, X.-L. Sun

Recent developments in carbohydrate-decorated targeted drug/gene delivery

Med Res Rev, 30 (2010), pp. 270–289

[26] K. Anderson, C. Fernandez, K.G. Rice

N-Glycan targeted gene delivery to the dendritic cell SIGN receptor

Bioconjug Chem, 21 (2010), pp. 1479–1485

[27] X. Yang, X. Yuan, D. Cai, S. Wang, L. Zong

Low molecular weight chitosan in DNA vaccine delivery via mucosa

Int J Pharm, 375 (2009), pp. 123–132

[28] I.Y. Park, I.Y. Kim, M.K. Yoo, Y.J. Choi, M.-H. Cho, C.S. Cho

Mannosylated polyethylenimine coupled mesoporous silica nanoparticles for receptor-mediated gene delivery

Int J Pharm, 359 (2008), pp. 280–287

[29] Y. Lu, S. Kawakami, F. Yamashita, M. Hashida

Development of an antigen-presenting cell-targeted DNA vaccine against melanoma by mannosylated liposomes

Biomaterials, 28 (2007), pp. 3255–3262

[30] C. Kieburg, T.K. Lindhorst

Glycodendrimer synthesis without using protecting groups

Tetrahedron Lett, 38 (1997), pp. 3885–3888

[31] G. Li, H. Tarima, T. Ohtani

An improved procedure for the preparation of isothiocyanates from primary amines by using hydrogen peroxide as the dehydrosulfurization reagent

J Org Chem, 62 (1997), pp. 4539–4540

[32] J.M. Benito, M. Gómez-García, C. Ortiz Mellet, I. Baussanne, J. Defaye, J.M. García Fernández

Optimizing saccharide-directed molecular delivery to biological receptors: design, synthesis, and biological evaluation of glycodendrimer-cyclodextrin conjugates

J Am Chem Soc, 126 (2004), pp. 10355–10363

[33] J.W. Tilley, P. Levitan, R.W. Kierstead, M. Cohen

Antihypertensive (2-aminoethyl)thiourea derivatives

1 J Med Chem, 23 (1980), pp. 1387–1392

[34] J.L. Jiménez Blanco, P. Bootello, C. Ortiz Mellet, R. Gutiérrez Gallego, J.M. García Fernández

The synthesis and structure of linear and dendritic thiourea-linked glycooligomers

Eur J Org Chem (2006), pp. 183–196

[35] M.-H. Louis, S. Dutoit, Y. Denoux, P. Erbacher, E. Deslandes, J.-P. Behr et al.

Intraperitoneal linear polyethylenimine (L-PEI)-mediated gene delivery to ovarian carcinoma nodes in mice

Cancer Gene Ther, 13 (2006), pp. 367–674

[36] O. Boussif, F. Lezoualc'h, M.A. Zanta, M.D. Mergny, D. Scherman, B. Demeneix et al.

A versatile vector for gene and oligonucleotide transfer into cells in culture and in vivo: Polyethylenimine

Proc Natl Acad Sci U S A, 92 (1995), pp. 7297–7301

[37] I. Baussanne, J.M. Benito, C. Ortiz Mellet, J.M. García Fernández, J. Defaye

Dependence of concanavalin A binding on anomeric configuration, linkage type, and ligand multiplicity for thiourea-bridged mannopyranosyl-β-cyclodextrin conjugates

ChemBioChem, 2 (2001), pp. 777–783

[38] R. Euzen, J.-L. Reymond

Glycopeptide dendrimers: tuning carbohydrate–lectin interactions with amino acids

Mol Biosyst, 7 (2011), pp. 411–421

[39] C.D. Muller, F. Schuber

Neo-mannosylated liposomes: synthesis and interaction with mouse Kupffer cells and resident peritoneal macrophages

Biochim Biophys Acta, 986 (1989), pp. 97–105

[40] L. Desigaux, M. Sainlos, O. Lambert, R. Chevre, E. Letrou-Bonneval, J.-P. Vigneron et al.

Self-assembled lamellar complexes of siRNA with lipidic aminoglycoside derivatives promote efficient siRNA delivery and interference

Proc Natl Acad Sci U S A, 104 (2007), pp. 16534–16539

[41] J.L. Jiménez Blanco, P. Bootello, J.M. Benito, C. Ortiz Mellet, J.M. García Fernández

Urea-, thiourea-, and guanidine-linked glycooligomers as phosphate binders in water

J Org Chem, 71 (2006), pp. 5136–5143

[42] H. Bayley, D.N. Standring, J.R. Knowles

Propane-1,3-dithiol: a selective reagent for the efficient reduction of alkyl and aryl azides to amines

Tetrahedron Lett, 19 (1978), pp. 3633–3634

[43] J.L. Jiménez Blanco, P. Bootello, R. Gutiérrez-Gallego, C. Ortiz Mellet, J.M. García Fernández

Synthesis of thiourea-linked glycooligomers that mimic the branching patterns of natural oligosaccharides

Synthesis (Stuttg) (2007), pp. 2545–2558

[44] M. Lahmann

Top Curr Chem, 288 (2009), pp. 17–65

[45] M. Gómez-García, J.M. Benito, R. Gutiérrez-Gallego, A. Maestre, C. Ortiz Mellet, J.M. García Fernández et al.

Comparative studies on lectin–carbohydrate interactions in low and high density homo- and heteroglycoclusters

Org Biomol Chem, 8 (2010), pp. 1849–1860

[46] B. Halvorsen, U.K. Aas, M.A. Kulseth, C.A. Drevon, E.N. Christiansen, S.O. Kolset

Proteoglycans in macrophages: characterization and possible role in the cellular uptake of lipoproteins

Biochem J, 331 (1998), pp. 743–752

[47] P.D. Stahl, J.S. Rodman, M.J. Miller, P.H. Schlesinger

Evidence for receptor-mediated binding of glycoproteins, glycoconjugates, and lysosomal glycosidases by alveolar macrophages

Proc Natl Acad Sci U S A, 75 (1978), pp. 1399–1403

Figure captions

Figure 1. Schematic representation of cyclodextrins (CDs), polycationic amphiphilic CDs (paCDs; left), polycationic glyco-amphiphilic CDs (pGaCDs; right), the corresponding nanocomplexes with pDNA (CDplexes and GlycoCDplexes, respectively) and their presumed internalization routes.

Figure 2. Structures of the polycationic amphiphilic CD (paCD) 1 [21], the glyco-amphiphilic CD (GaCD) 2 and the polycationic glyco-amphiphilic CDs (pGaCDs) 3 and 4.

Figure 3. TEM micrograph of 3:pDNA CDplexes with amplification of the ultrathin structure of the particles and a schematic representation of the proposed arrangement of pGaCDs and DNA strains.

Figure 4. Inhibition of Con A (dashed lines) and MMR (solid lines) binding to yeast mannan by increasing amounts of 1:pDNA (●), 3:pDNA (▲) and 4:pDNA (■) CDplexes at N/P 5. Data for 1:pDNA-ConA and 4:pDNA-MMR (no inhibition for any on them) are omitted for clarity.

Figure 5. (A) Adhesion to mice peritoneal macrophages of nanocomplexes obtained from 1, 3 and 4 vs. naked pDNA and PEI (25 kDa) at N/P 5 (blank bars) and 10 (solid bars). (B) Adhesion data at N/P 5 in the absence (blank bars) and in the presence of mannosylated-BSA (1 mg mL−1, dotted bars) or native BSA (1 mg mL−1, stripped bars).

Figure 6. Transfection efficiency (bars) and cell viability (●) in RAW 264.7 cells for N/P 5 CDplexes obtained from 1, 3 and 4 vs. naked pDNA in the absence (blank bars) and in the presence (solid bars) of yeast mannan (5 mg mL−1).

Figure 7. FACS monitoring of the uptake of 3:pDNA CDplexes at N/P 5 in RAW264.7 cells: (A) control, (B) 3:pDNA, (C) 3:pDNA + yeast mannan (5 mg mL−1), and (D) overall representation featuring control (black), 3:pDNA (blue), and 3:pDNA + yeast mannan (green) lines (For interpretation of the references to colour in this figure legend, the reader is referred to the web version of this article.)

Figure 8. Transfection efficiency achieved with 1:pDNA and 3:pDNA CDplexes at N/P 5 vs. naked pDNA in RAW 264.7 (A) and BNL-CL2 cells (B) in the absence (white bars) and in the presence (grey bars) of yeast mannan (5 mg mL−1).

Table 1

Table 1. Size (hydrodynamic diameter, nm) and ζ-potential (mV) of CDplexes (N/P 10) determined by DLS and M3-PALS analysis, respectively.

Complex	**av. diameter (nm)**	**ζ–potential (mV)**
1:pDNA	76 ± 10	46.1 ± 1
3:pDNA	80 ± 35	40 ± 1
4:pDNA	100 ± 20	48 ± 1

Figure 1

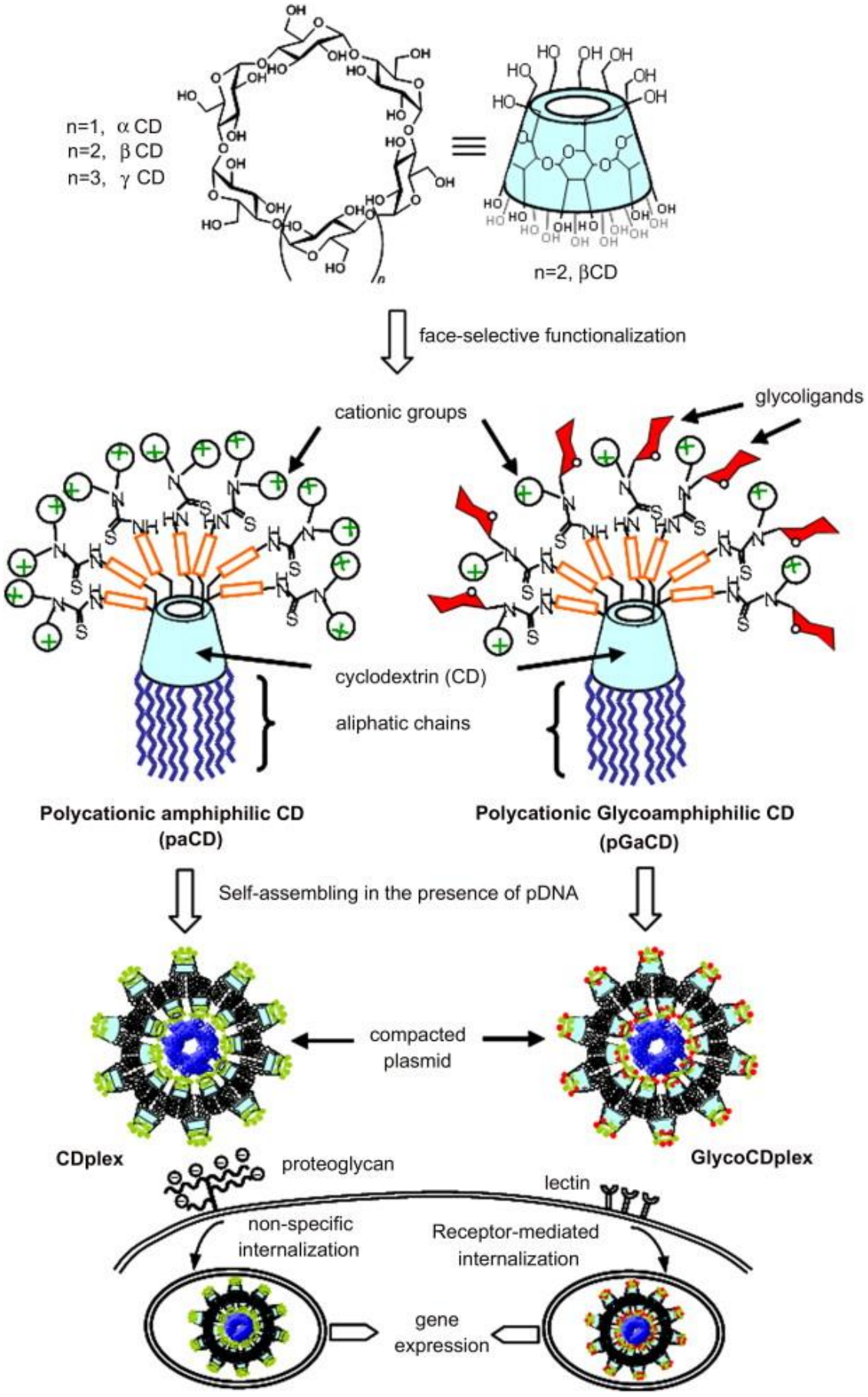
n=1, α CD
n=2, β CD
n=3, γ CD
n=2, βCD
face-selective functionalization
cationic groups
glycoligands
cyclodextrin (CD)
aliphatic chains
Polycationic amphiphilic CD
(paCD)
Polycationic Glycoamphiphilic CD
(pGaCD)
Self-assembling in the presence of pDNA
compacted
plasmid
CDplex
GlycoCDplex
proteoglycan
lectin
non-specific
internalization
Receptor-mediated
internalization
gene
expression

Figure 2

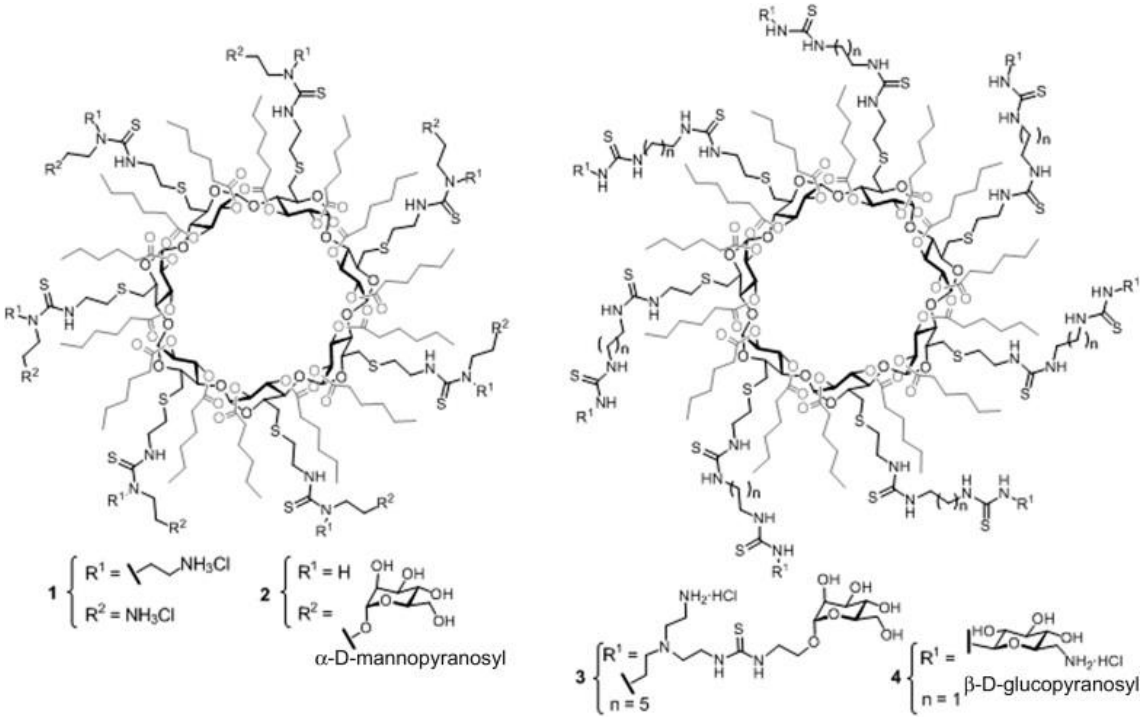
1
R1 = NH3Cl
R2 = NH3Cl
2
R1 = H
R2 =
α-D-mannopyranosyl
3
R1 =
n = 5
4
R1 =
n = 1
β-D-glucopyranosyl

Figure 3

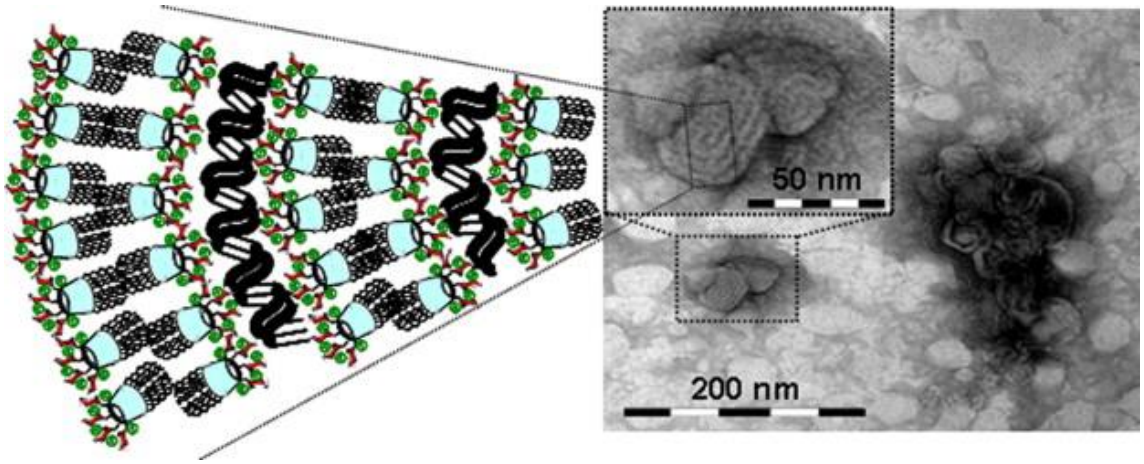

Figure 4

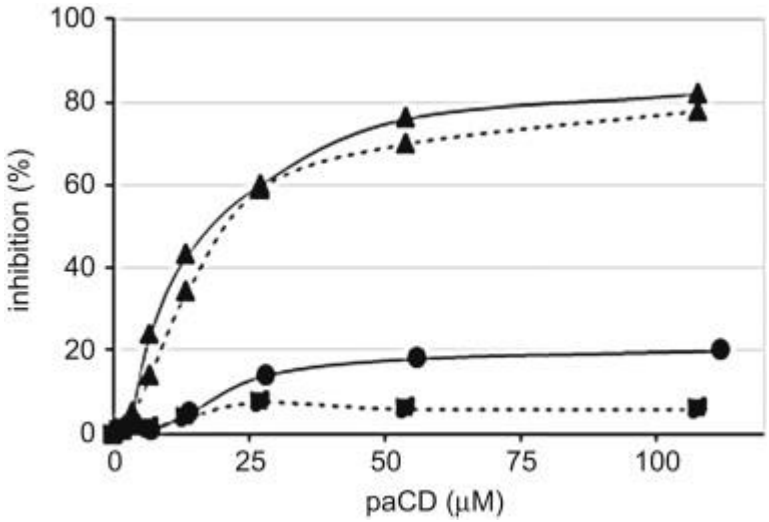

Figure 5

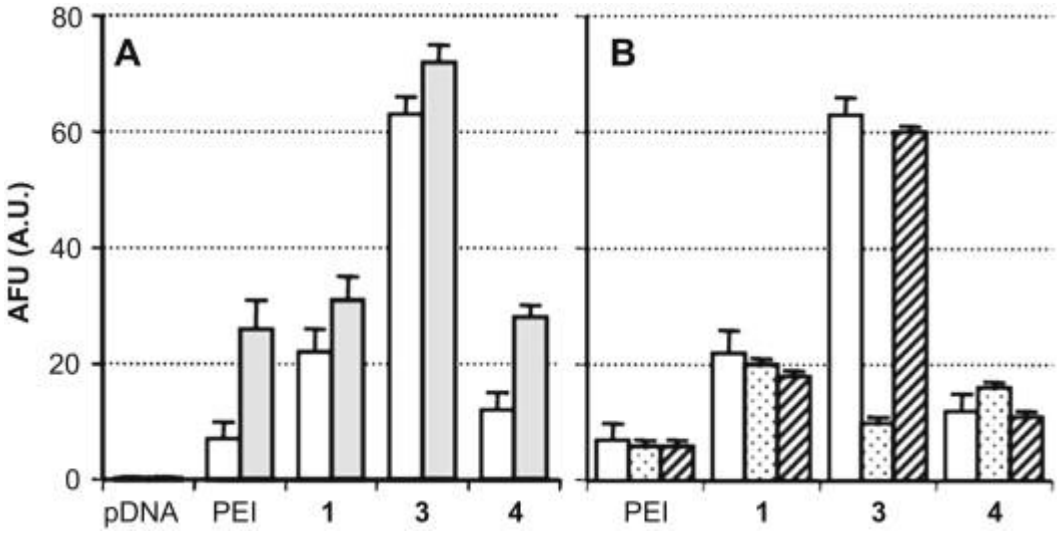

Figure 6

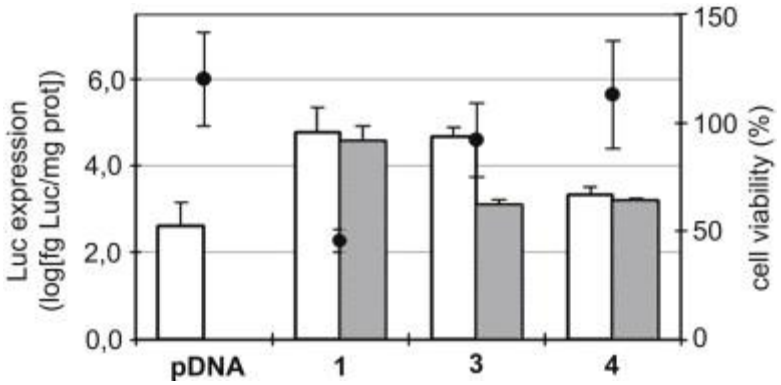
Luc expression
(log[fg Luc/mg prot])
6,0
4,0
2,0
0,0
150
100
50
0
cell viability (%)
pDNA
1
3
4

Figure 7

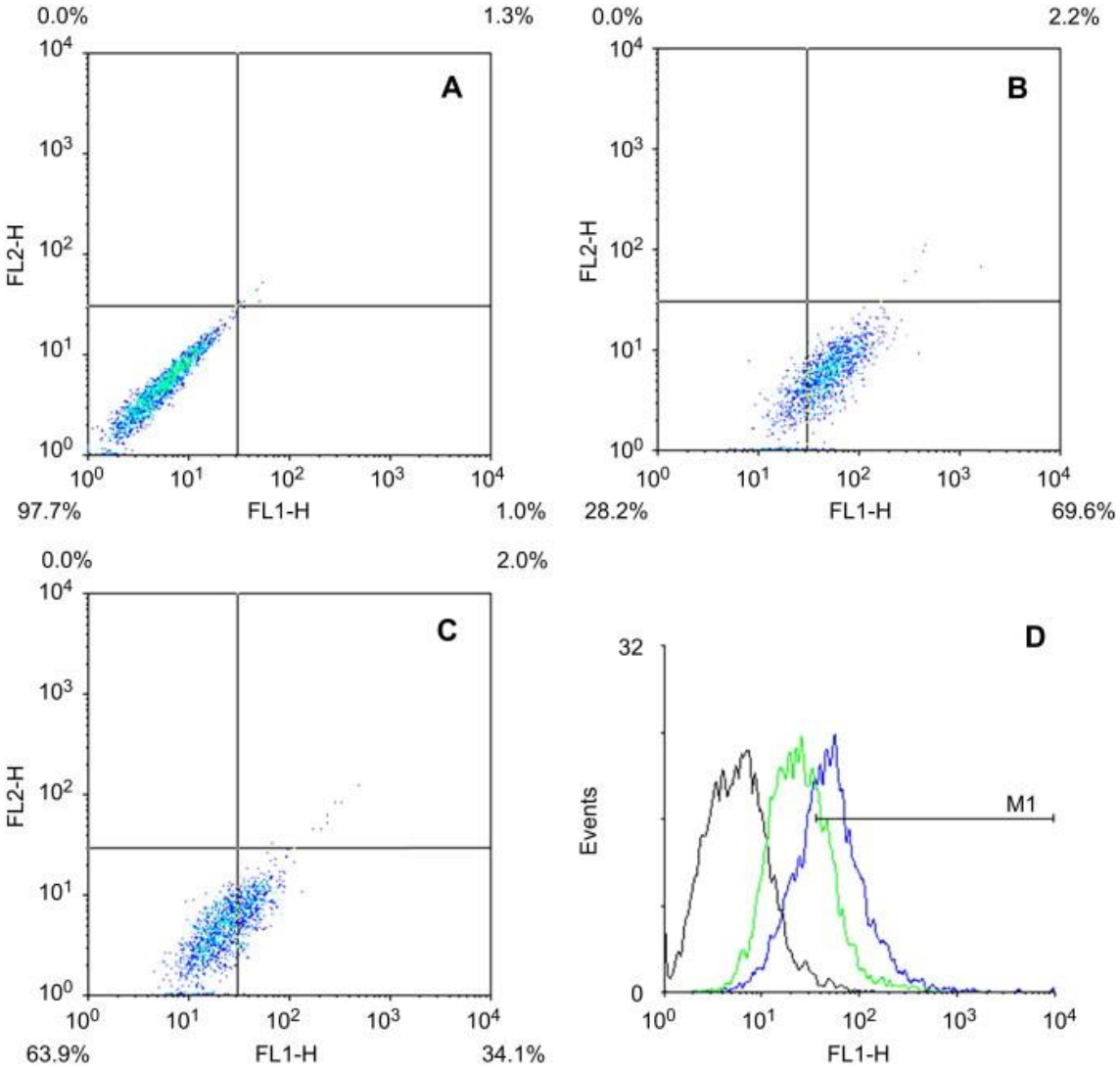
A
0.0%
1.3%
97.7%
1.0%
B
0.0%
2.2%
28.2%
69.6%
C
0.0%
2.0%
63.9%
34.1%
D
32
0
Events
M1
FL1-H
FL2-H

Figure 8

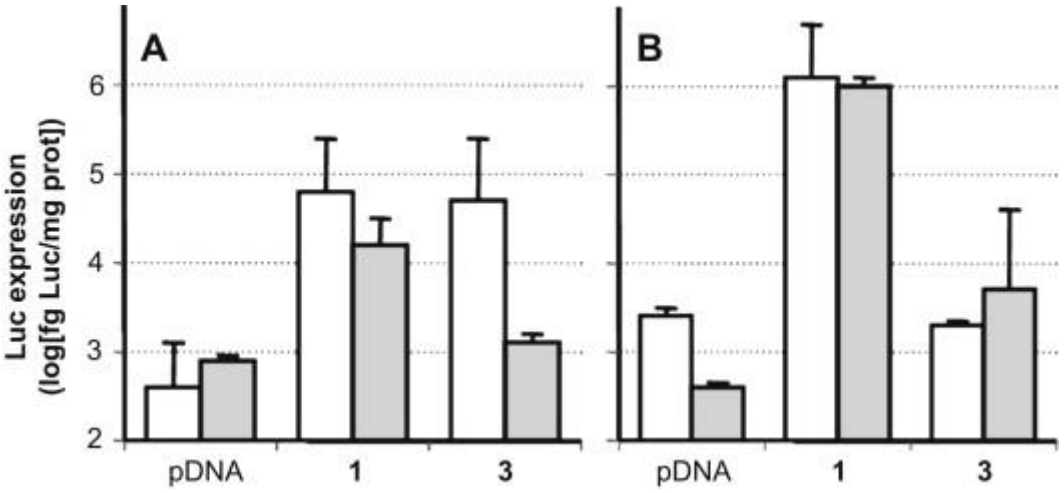

Scheme 1

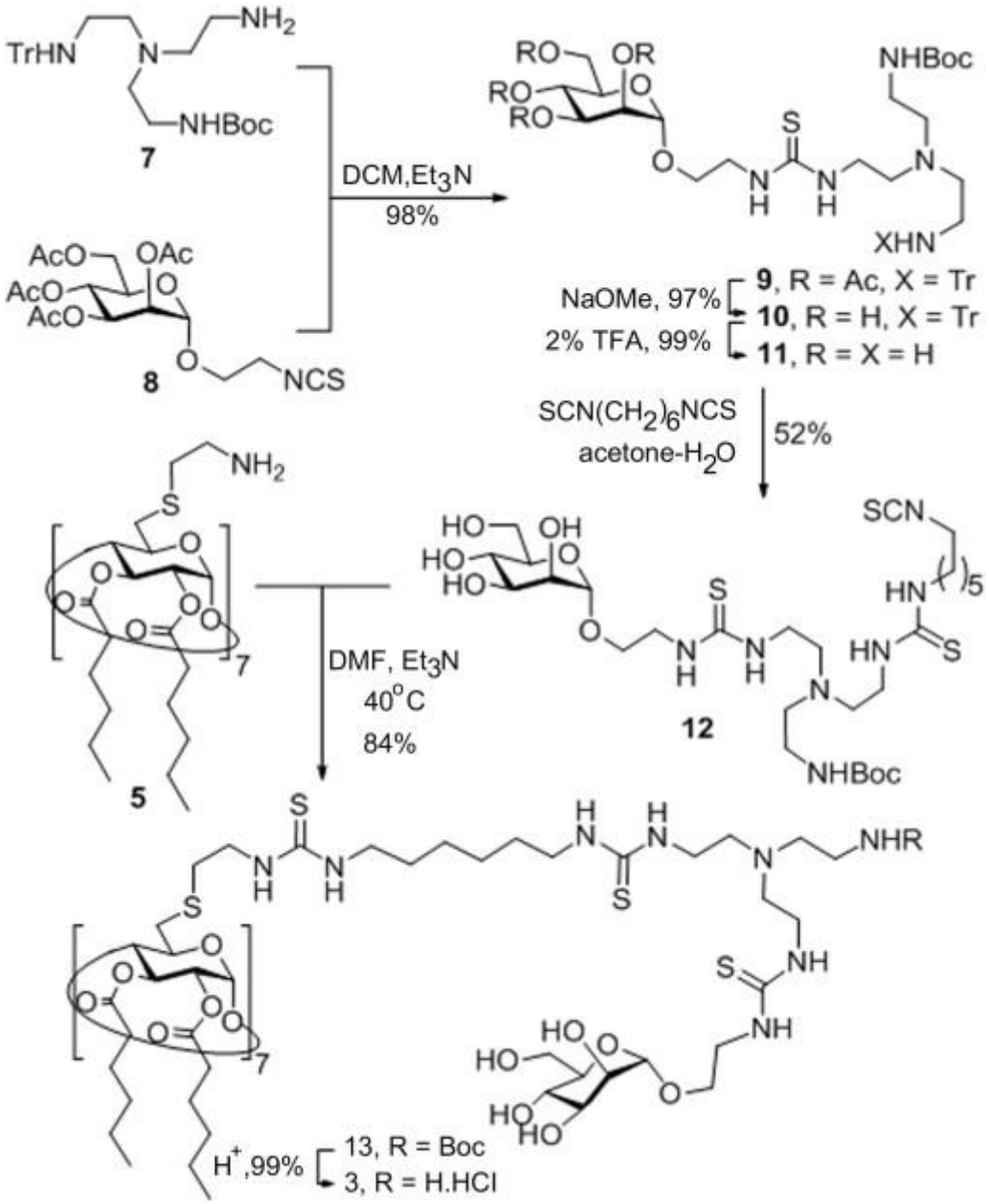

Scheme 1. Synthesis of pGaCD 3.

Scheme 2

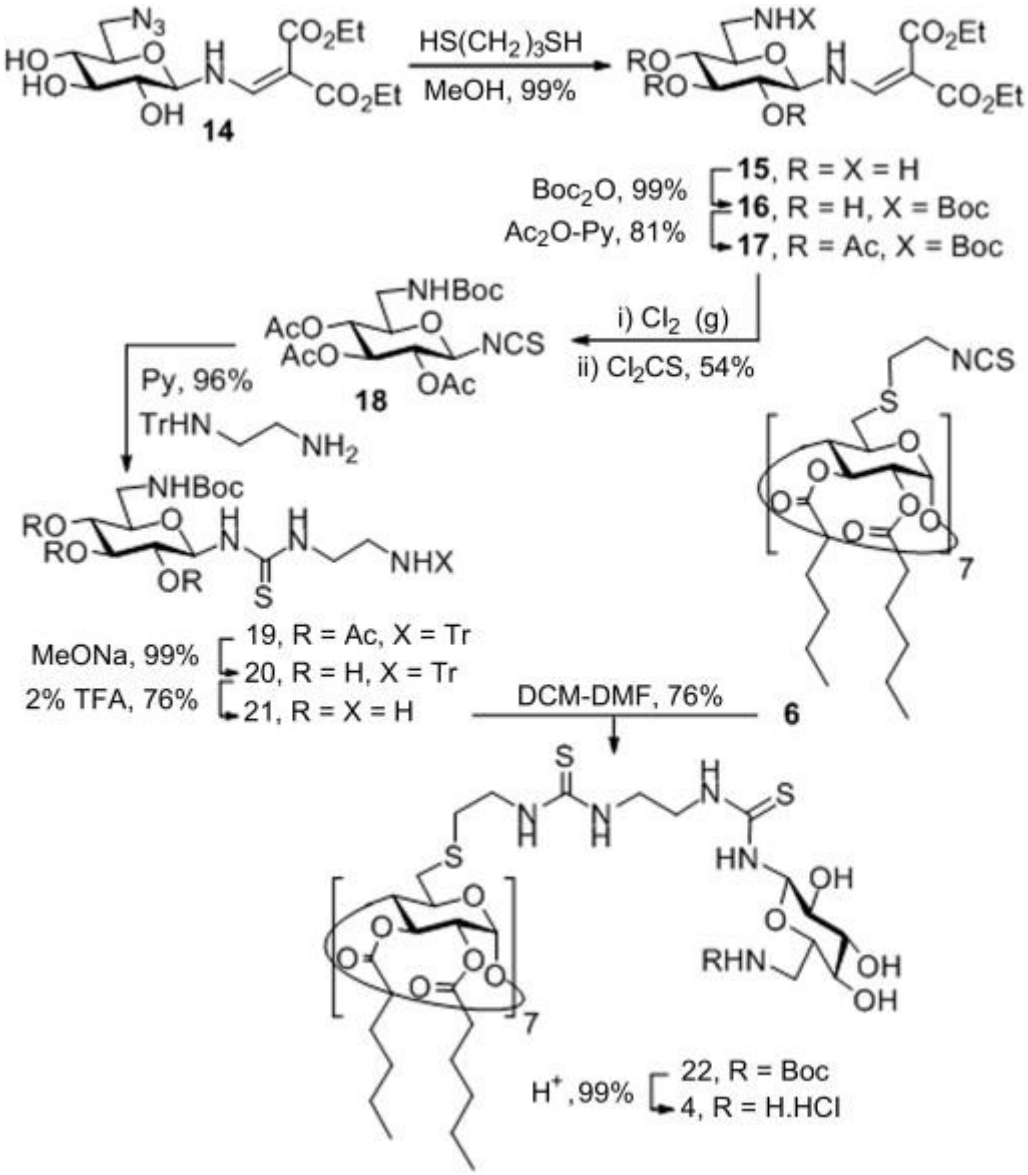

Scheme 2. Synthesis of pGaCD 4.